

Lecture-5

CSO202: Atoms, Photons & Molecules

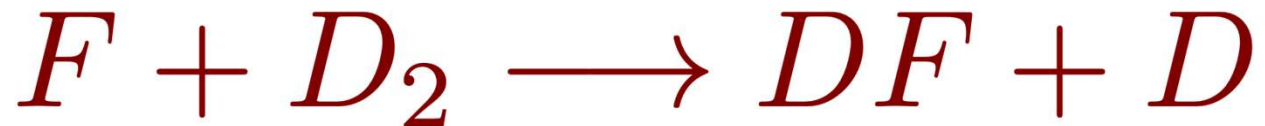
Debabrata Goswami

Molecular beam studies of the F+D₂ and F+HD reactions

D. M. Neumark,^{a)} A. M. Wodtke, G. N. Robinson, C. C. Hayden,^{b)} K. Shobatake,^{c)} R. K. Sparks,^{d)} T. P. Schafer, and Y. T. Lee

Materials and Molecular Research Division, Lawrence Berkeley Laboratory and Department of Chemistry, University of California, Berkeley, California 94720

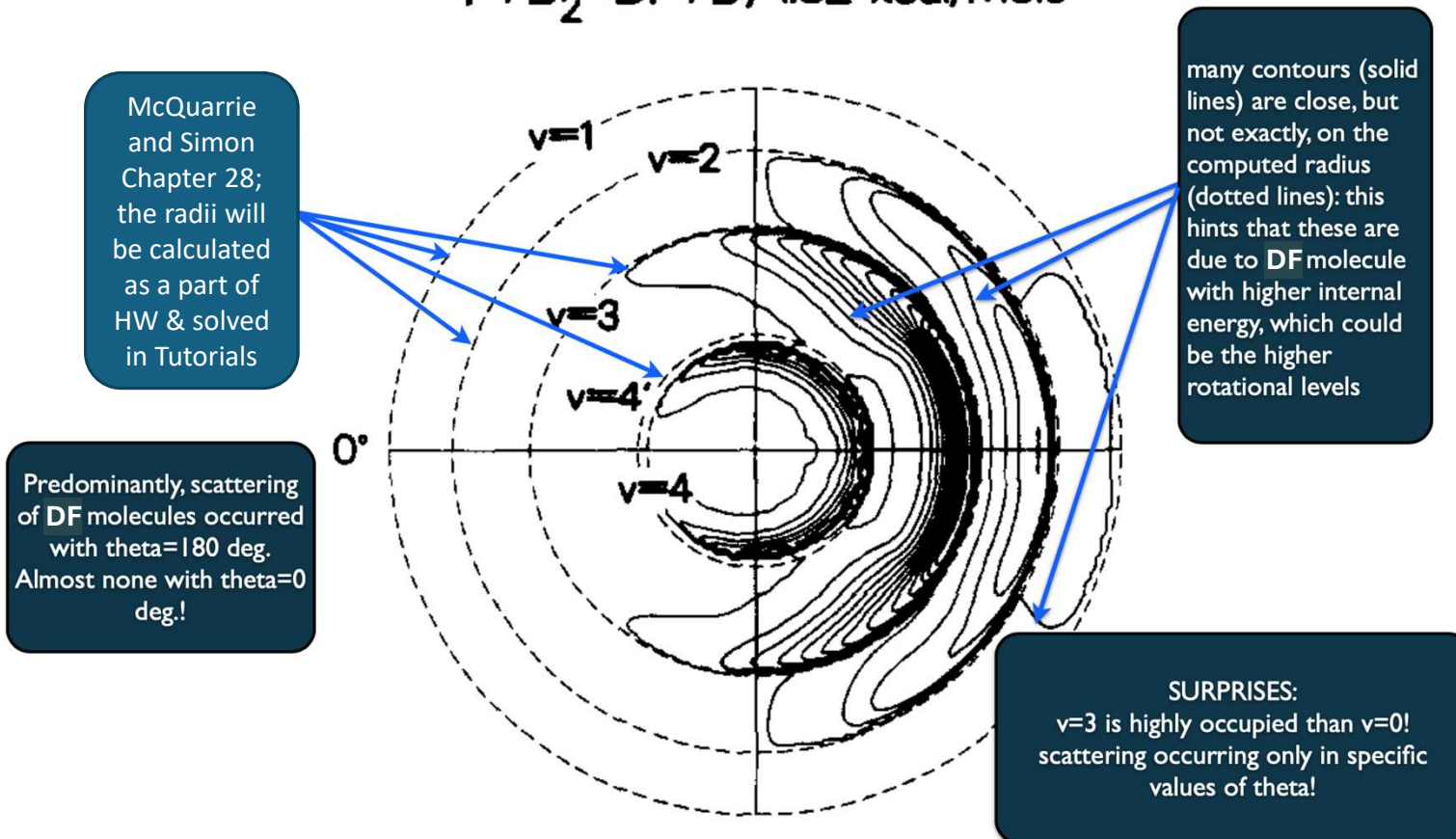
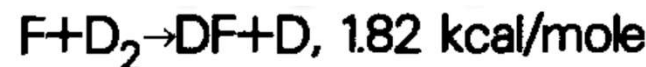
(Received 27 August 1984; accepted 13 November 1984)



Quantum state-specific study!

Does rate depend on how vibrationally excited D₂ is?

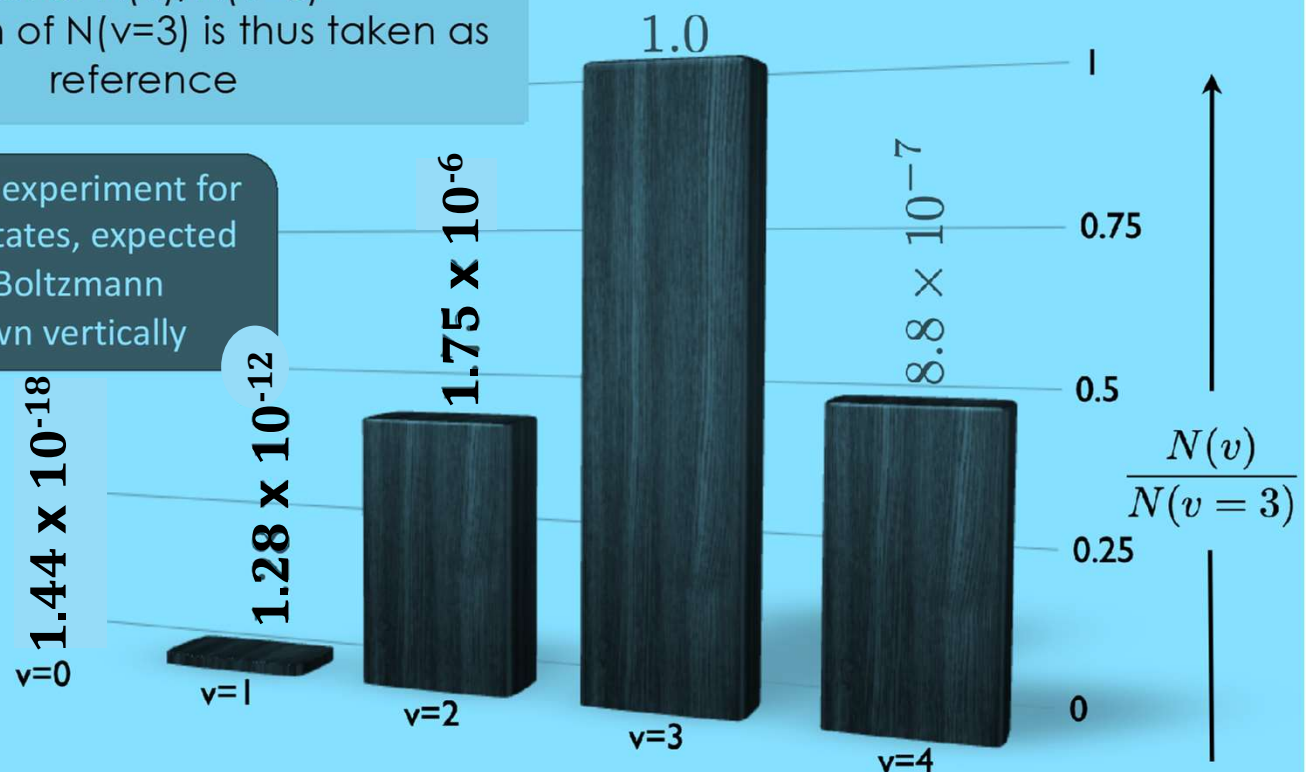
Newton Diagram from JCP (1985)



Population of Vibrational States

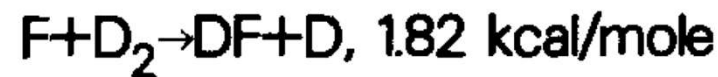
Plot of $N(v)/N(v=3)$
Population of $N(v=3)$ is thus taken as reference

Population from Lee's experiment for different vibrational states, expected population from Boltzmann distribution is shown vertically

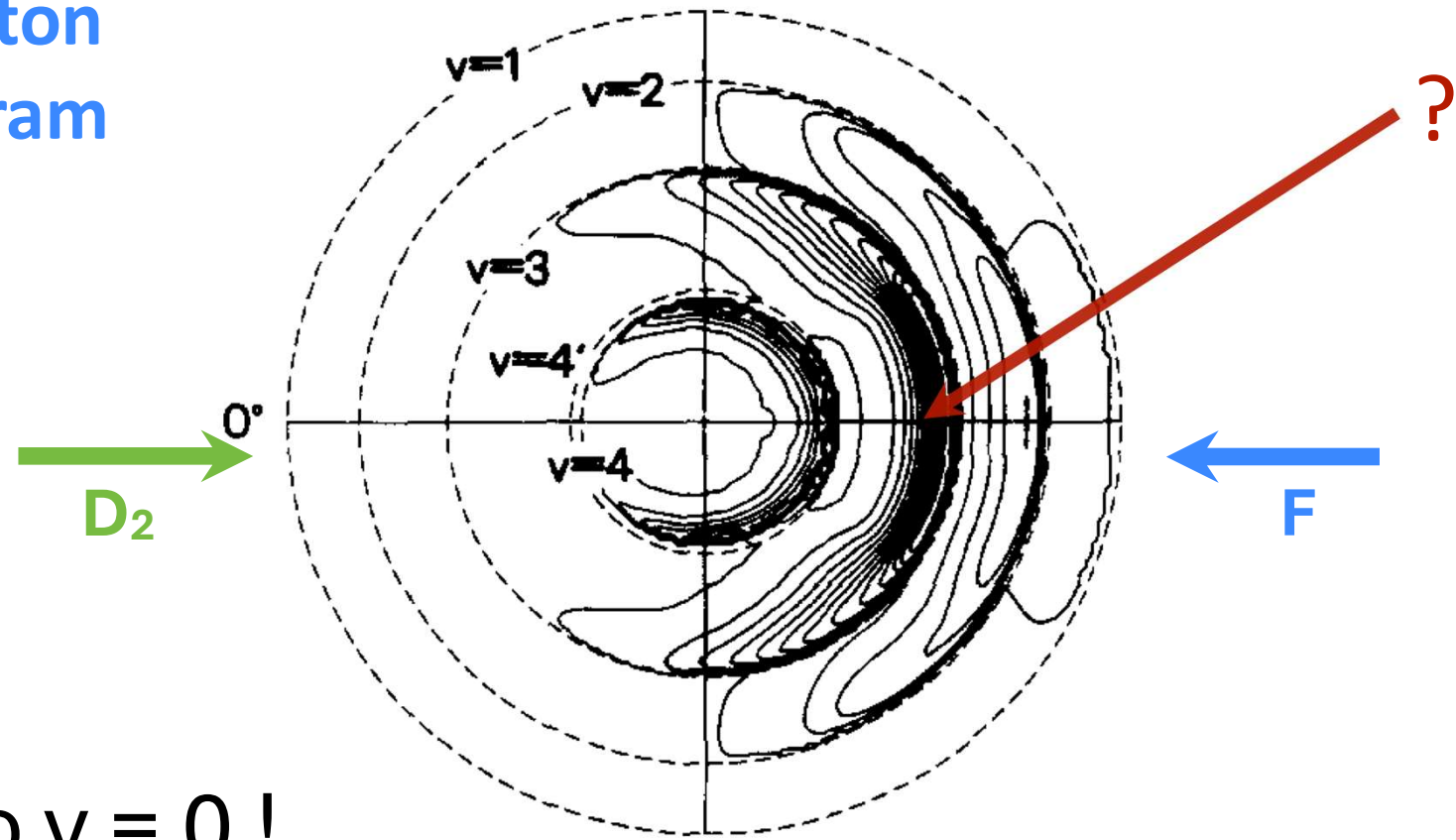


population of vibrational states is not Boltzmann distributed where one expects higher population for the lowest energy state, and exponentially decreasing population for higher energy states

DF molecules are not in equilibrium!

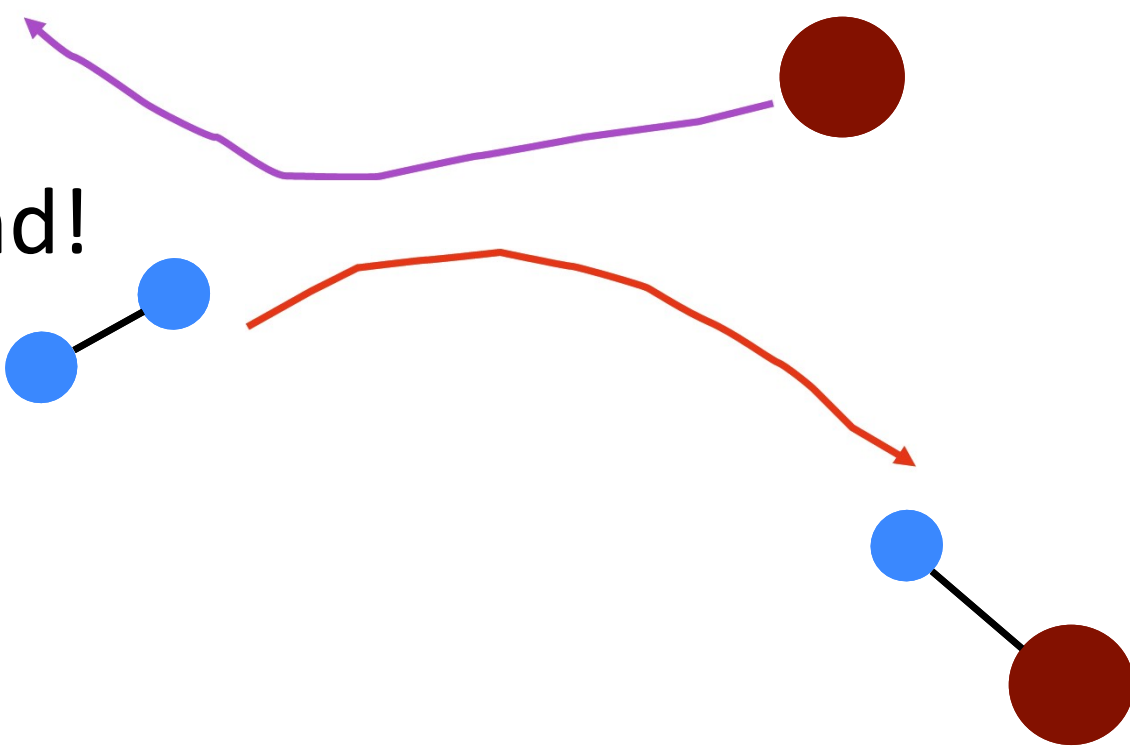


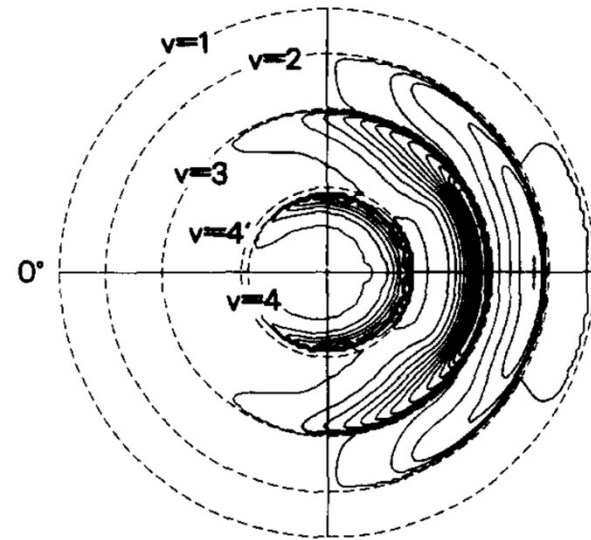
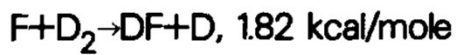
Newton
diagram



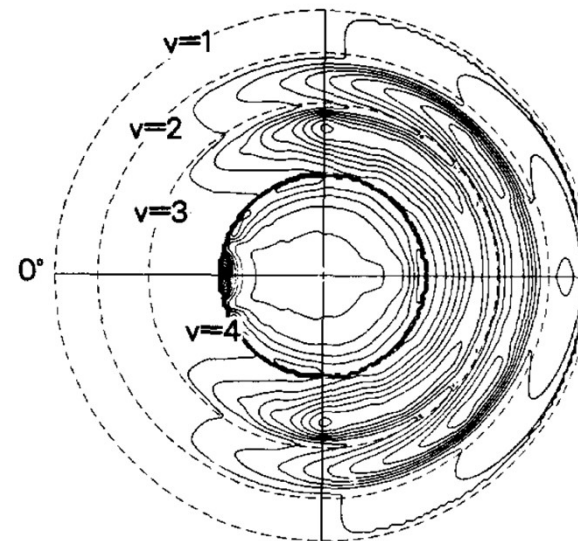
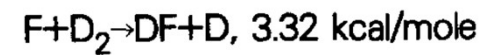
No $v = 0$!

Rebound!





Rebound



Some Forward-Flux seen

Collision energy matters!

Mysteries of Lee's Experiments which we would like to solve:

1. Why is the $D_2 + F$ reaction rebound?
2. Why is there a forward flux seen when the collision energy is increased? Why is this forward flux only observed for $v=4$?
3. Why is the population of the DF products higher for $v=3$ (and $v=4$ for some collisional energy)?

CHAPTER 28

PHYSICAL CHEMISTRY A MOLECULAR APPROACH

Donald A. McQuarrie • John D. Simon



1997 Edition

Gas-Phase Reaction Dynamics

Bimolecular gas-phase reactions are among the simplest elementary kinetic processes that occur in nature. In this chapter, we will examine some of the current models that are used to describe the molecular aspects of bimolecular gas-phase reactions. First, we will modify the collision theory presented in Chapter 25 and define the rate constant in terms of a reaction cross section. We will then examine experimentally measured reaction cross sections for several gas-phase reactions. The simplest gas-phase reaction is the hydrogen exchange reaction $H_A + H_B - H_C \Rightarrow H_A - H_B + H_C$. This reaction has been studied in great detail and the experimental data for it are often used to test theories of gas-phase chemical reactions.

In this chapter, however, we have chosen to focus our discussion on the reaction $F(g) + D_2(g) \Rightarrow DF(g) + D(g)$. From a study of this reaction, we will not only learn the same concepts that underlie the $H(g) + H_2(g)$ exchange reaction but will also learn about molecular processes that can occur in reactions in which $\Delta_r U^\circ < 0$. The reaction $F(g) + D_2(g)$ therefore serves as an excellent system for studying the molecular details of gas-phase reactions. We will examine data obtained from crossed molecular beam spectroscopy experiments and learn how such measurements reveal the chemical dynamics of reactive collisions. We will then see that contemporary quantum-mechanical calculations can provide a detailed description of the reaction path by which the $F(g) + D_2(g)$ reactants become the $DF(g) + D(g)$ products.

28-1. The Rate of a Bimolecular Gas-Phase Reaction Can Be Calculated Using Hard-Sphere Collision Theory and an Energy-Dependent Reaction Cross Section

The rate of the general bimolecular elementary gas-phase reaction



is given by

$$v = -\frac{d[A]}{dt} = k[A][B] \quad (28.2)$$

Hard-sphere collision theory can be used to estimate the rate constant k . Using the naive assumption that every collision between the hard spheres A and B yields products, the rate of reaction is given by the collision frequency per unit volume (Equation 25.57)

$$v = Z_{AB} = \sigma_{AB} \langle u_r \rangle \rho_A \rho_B \quad (28.3)$$

In Equation 28.3, σ_{AB} is the hard-sphere collision cross section of A and B molecules, $\langle u_r \rangle$ is the average relative speed of a colliding pair of A and B molecules, and ρ_A and ρ_B are the number densities of A and B molecules in the sample, respectively. Recall from Section 25–6 that the hard-sphere collision cross section σ_{AB} is given by $\sigma_{AB} = \pi d_{AB}^2$, where d_{AB} is the sum of the radii of the two colliding spheres. Being a collision frequency per unit volume, Z_{AB} has the units of collisions· $\text{m}^{-3}\cdot\text{s}^{-1}$, where the “units” collisions is not usually included. Because we are assuming that every collision leads to a reaction, Z_{AB} also gives us the number of product molecules formed per unit volume per unit time. Comparison of Equations 28.2 and 28.3 shows that we can define the rate constant as

$$k = \sigma_{AB} \langle u_r \rangle \quad (28.4)$$

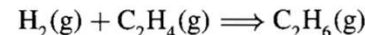
The units of k are given by the units of $Z_{AB}/\rho_A \rho_B$, or $\text{molecules} \cdot \text{m}^{-3} \cdot \text{s}^{-1}/(\text{molecules} \cdot \text{m}^{-3})^2 = \text{molecules}^{-1} \cdot \text{m}^3 \cdot \text{s}^{-1}$. To obtain k in the more commonly used units of $\text{dm}^3 \cdot \text{mol}^{-1} \cdot \text{s}^{-1}$, we need to multiply the right side of Equation 28.4 by N_A and by $(10 \text{ dm} \cdot \text{m}^{-1})^3$, giving

$$k = (1000 \text{ dm}^3 \cdot \text{m}^{-3}) N_A \sigma_{AB} \langle u_r \rangle \quad (28.5)$$

where σ_{AB} has units of m^2 and $\langle u_r \rangle$ has units of $\text{m} \cdot \text{s}^{-1}$.

EXAMPLE 28-1

Use hard-sphere collision theory to calculate the rate constant for the reaction



at 298 K. Express the rate constant in units of $\text{dm}^3 \cdot \text{mol}^{-1} \cdot \text{s}^{-1}$.

SOLUTION: The hard-sphere collision theory rate constant in units of $\text{dm}^3 \cdot \text{mol}^{-1} \cdot \text{s}^{-1}$

$$\begin{aligned} k &= (1000 \text{ dm}^3 \cdot \text{m}^{-3})(6.022 \times 10^{23} \text{ mol}^{-1})(3.85 \times 10^{-19} \text{ m}^2)(1.83 \times 10^3 \text{ m} \cdot \text{s}^{-1}) \\ &= 4.24 \times 10^{11} \text{ dm}^3 \cdot \text{mol}^{-1} \cdot \text{s}^{-1} \end{aligned}$$

The experimental rate constant for this reaction at 298 K is $3.49 \times 10^{-26} \text{ dm}^3 \cdot \text{mol}^{-1} \cdot \text{s}^{-1}$, more than 30 orders of magnitude smaller than the hard-sphere collision theory prediction!

We make our first improvement to collision theory by taking into account the dependence of the reaction rate on the relative speed, or the energy, of the collision.



28–6. Reactive Collisions Can Be Studied Using Crossed Molecular Beam Machines

One of the most important experimental techniques used to study the molecular dynamics of bimolecular gas-phase reactions is the *crossed molecular beam method*. The basic design of a crossed molecular beam apparatus is shown in Figure 28.6a. The experimental device is designed to cross a beam of A molecules with a beam of B molecules at a specific location inside a large vacuum chamber. The product molecules are then detected using a mass spectrometer. In some crossed molecular beam machines, the detector can be rotated in the plane defined by the two molecular beams, thereby allowing the measurement of the angular distribution of the scattered products. The mass spectrometer can also be set to measure a specific molecular mass so that individual product molecules are detected.

Supersonic molecular beams are used to produce the velocities of the molecules in the reactant beams. A schematic diagram of a supersonic molecular beam source is shown in Figure 28.6b. A supersonic molecular beam can be generated by taking a high-pressure, dilute mixture of the reactant molecule of interest in an inert carrier gas (He and Ne are commonly used) and pulsing the mixture through a small nozzle into the vacuum chamber. A small pinhole, known as a skimmer, is located a few centimeters away from where the molecules enter the vacuum chamber through the nozzle. Only those molecules that pass through the small hole in the skimmer enter the remainder of the vacuum chamber. This procedure creates a collimated beam of molecules. The beam is supersonic because the pressure conditions inside the vacuum chamber are such that the molecules in the beam move at a speed greater than the speed of sound

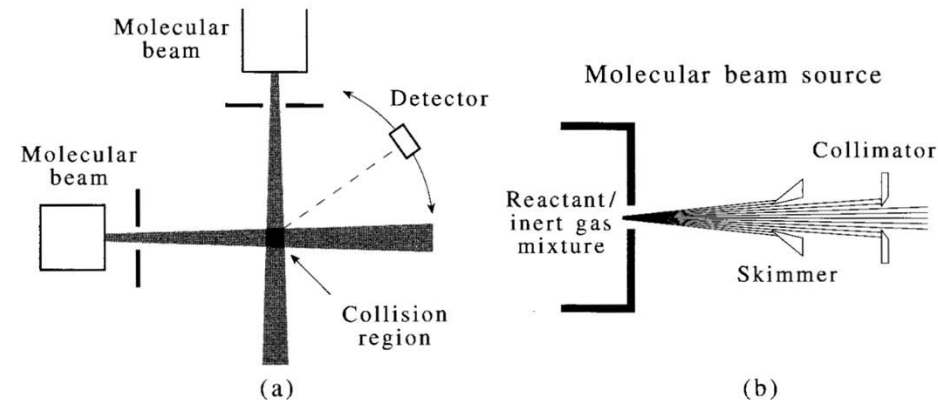


FIGURE 28.6

(a) A schematic diagram of a crossed molecular beam machine. Each reactant is introduced into the vacuum chamber by a molecular beam source. The two molecular beams collide at the collision region. The product molecules then travel away from the collision region. A mass spectrometer detector is located at a fixed distance away from the collision region and is used to detect product molecules. The detector can be moved so that the number of molecules leaving the collision region at different angles can be determined. (b) A schematic drawing of a supersonic molecular beam source. The reactant is expanded along with an inert gas through a small orifice into the vacuum chamber. A skimmer is used so that a collimated beam of molecules is directed toward the collision region.

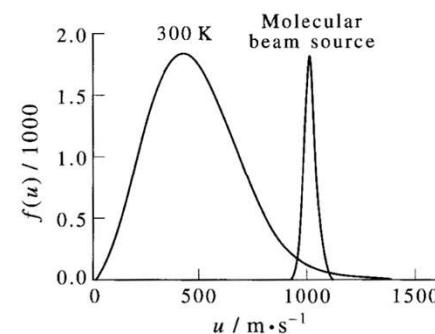


FIGURE 28.7

The Maxwell-Boltzmann velocity distribution of $\text{N}_2(\text{g})$ molecules at 300 K is compared with the velocity distribution generated by a supersonic expansion of a gaseous mixture of $\text{N}_2(\text{g})$ in He(g) at 300 K. The molecular beam produces a narrow, nonequilibrium velocity distribution.

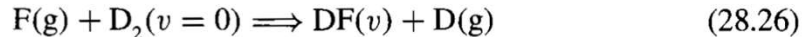
28-7. The Reaction $F(g) + D_2(g) \Rightarrow DF(g) + D(g)$ Can Produce vibrationally Excited $DF(g)$ Molecules

In this and several of the following sections, we will be concerned with the reaction



Figure 28.8 shows a one-dimensional energy diagram for this reaction. The energy diagram reflects only the changes in potential energy. Diagrams that indicate how the potential energy changes as the reaction proceeds along the reaction coordinate are called *potential energy diagrams*. The energy of the lowest vibrational state of $D_2(g)$ and the energies of the first six vibrational states of $DF(g)$ are also shown. In drawing these energy states, we have assumed that the vibrational motion of both $D_2(g)$ and $DF(g)$ is harmonic.

We consider here the reaction energetics when the reactant $D_2(g)$ is in its ground vibrational state, with an internal energy of $(1/2)\hbar\nu_{D_2}$. Figure 28.8 shows that the reaction can produce $DF(g)$ in several of its low vibrational states. We will write the overall reaction as



where the vibrational state of the reaction is specified but the vibrational state(s) of the product is left unspecified and must be determined experimentally. The total energy available for the reaction, E_{tot} , is the sum of the internal energy of the reactants, E_{int} , and the relative translational energy of the reactants, E_{trans} . Because energy must be conserved,

$$E_{\text{tot}} = E_{\text{trans}} + E_{\text{int}} = E'_{\text{trans}} + E'_{\text{int}} \quad (28.27)$$

where E'_{int} and E'_{trans} are the internal energy (rotational, vibrational, and electronic) and relative translational energy of the product molecules, respectively. For a given total energy, a change in the internal energy of the products, E'_{int} , must be balanced by a corresponding change in their relative translational energy, E'_{trans} . Thus for a fixed total collision energy, $DF(g)$ molecules generated in different vibrational states move away from the collision region with different velocities. We will find it useful to consider separately the rotational, vibrational, and electronic contributions to E_{int} and E'_{int} . We can write Equation 28.27 as

$$E_{\text{tot}} = E_{\text{trans}} + E_{\text{rot}} + E_{\text{vib}} + E_{\text{elec}} = E'_{\text{trans}} + E'_{\text{rot}} + E'_{\text{vib}} + E'_{\text{elec}} \quad (28.28)$$

For the reaction given by Equation 28.26, where the reactants and products are in their ground electronic states, $E_{\text{elec}} = -D_e(D_2)$ and $E'_{\text{elec}} = -D_e(DF)$.

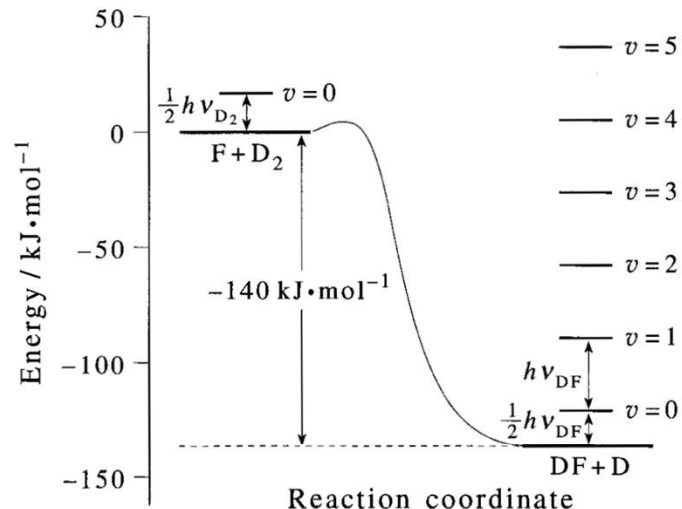
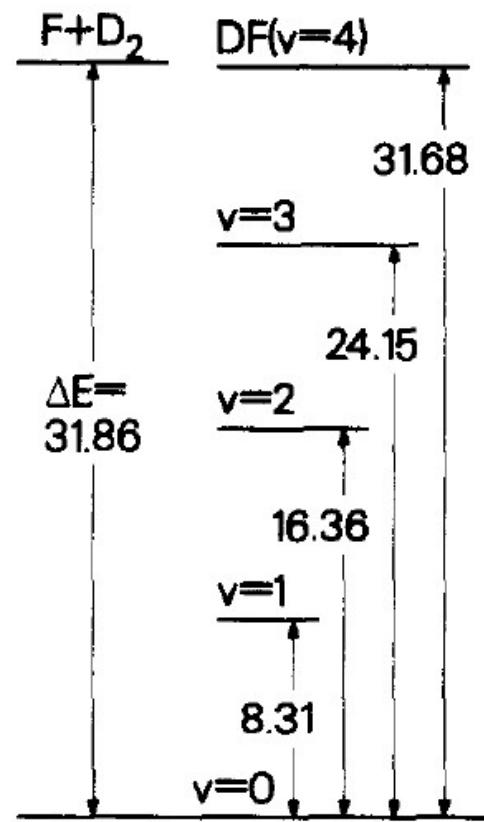
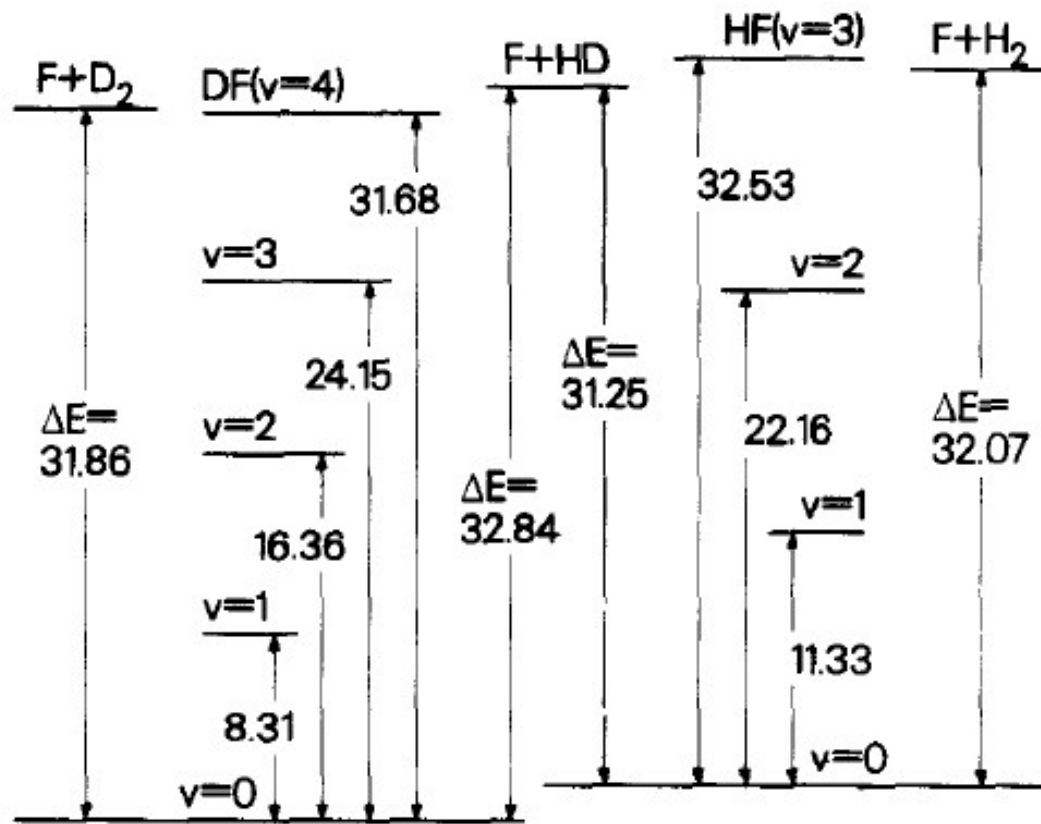
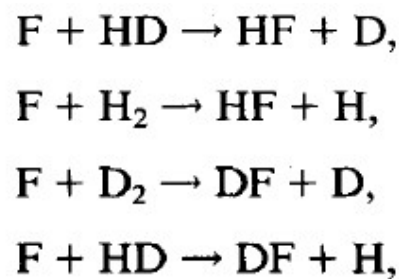


FIGURE 28.8

A potential-energy diagram for the reaction $F(g) + D_2(v = 0) \Rightarrow DF(v) + D(g)$. The vibrational states of the $D_2(g)$ reactant and $DF(g)$ product are indicated and labeled by their vibrational quantum numbers. The potential-energy diagram shows that the difference between the ground electronic state energies of $D_2(g)$ and $DF(g)$ is $D_e(D_2) - D_e(DF) = -140 \text{ kJ}\cdot\text{mol}^{-1}$. The reaction has an activation energy barrier of about $7 \text{ kJ}\cdot\text{mol}^{-1}$.

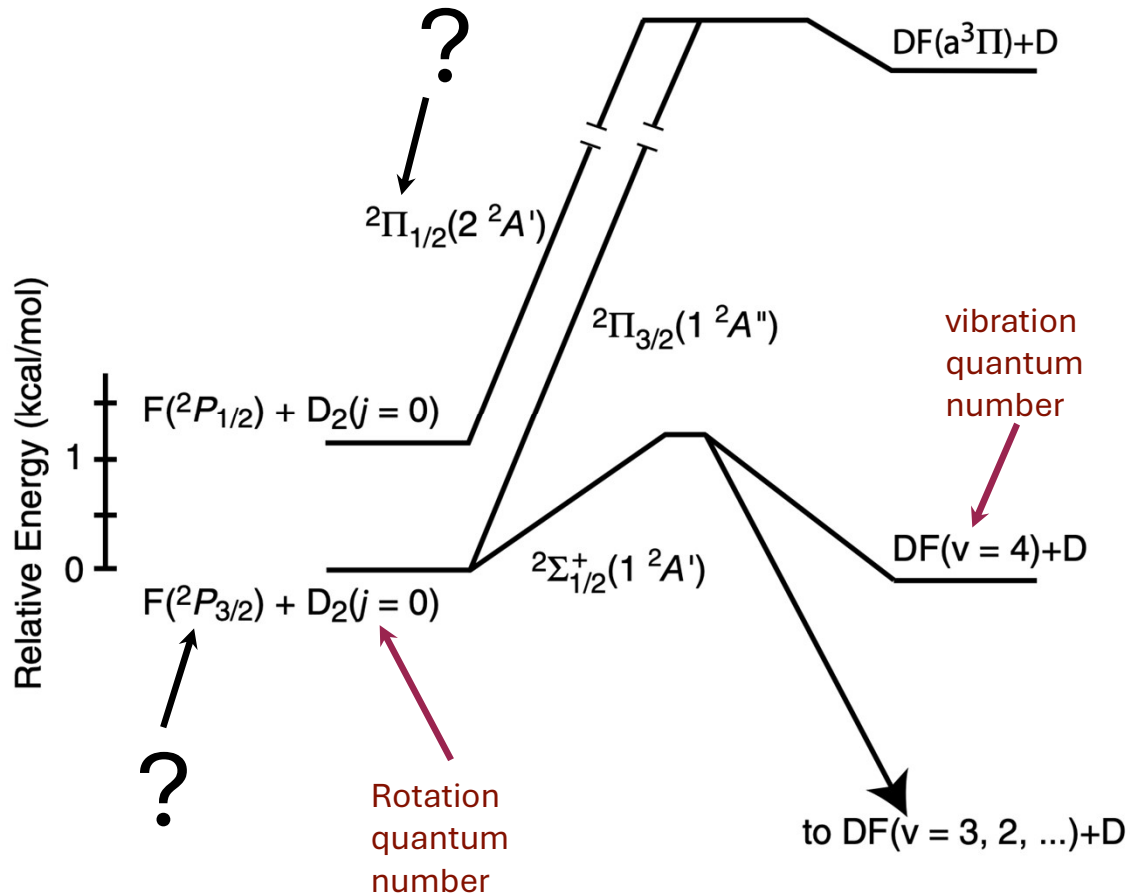


Energetics of the $F + D_2$ reactions. All values are in kcal/mol. D_2 is in its lowest internal states ($v = 0, J = 0$).



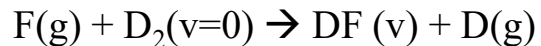
Energetics of the $\text{F} + \text{H}_2$, $\text{F} + \text{D}_2$, and $\text{F} + \text{HD}$ reactions. All values are in kcal/mol. H_2 , D_2 , and HD are in their lowest internal states ($v = 0, J = 0$).

Energetics



Homework Problem

1. Consider the reaction:



where the reactive translational energy of the reactants is 7.67 kJ.mol⁻¹. Assuming the reactants and products are in their ground electronic states and ground rotational states, determine the range of possible vibrational states of the product, DF(g). Treat the vibrational motion of both D₂(g) and DF(g) as harmonic with $\tilde{\nu}_{D_2} = 2990\text{ cm}^{-1}$ and $\tilde{\nu}_{DF} = 2907\text{ cm}^{-1}$. [$D_e(D_2) - D_e(DF) = 140\text{ kJ. mol}^{-1}$]

28–8. The Velocity and Angular Distribution of the Products of a Reactive Collision Provide a Molecular Picture of the Chemical Reaction

We will now examine the crossed molecular beam data for the reaction described by $\text{F(g)} + \text{D}_2(v = 0) \implies \text{DF}(v) + \text{D(g)}$ for the case in which the relative translational energy of the reactants is $7.62 \text{ kJ}\cdot\text{mol}^{-1}$. In Example 28–6, we found that for this value of the relative translational energy of the reactants, the product DF(g) could be produced in the vibrational states from $v = 0$ through $v = 4$.

28-8. The Velocity and Angular Distribution of the Products of a Reactive Collision Provide a Molecular Picture of the Chemical Reaction

We will now examine the crossed molecular beam data for the reaction described by $F(g) + D_2(v = 0) \rightarrow DF(v) + D(g)$ for the case in which the relative translational energy of the reactants is 7.62 $\text{kJ} \cdot \text{mol}^{-1}$. we found that for this value of the relative translational energy of the reactants, the product $DF(g)$ could be produced in the vibrational states from $v = 0$ through $v = 4$. We will now describe this reaction using the center-of-mass coordinate system presented in Section 28-5.

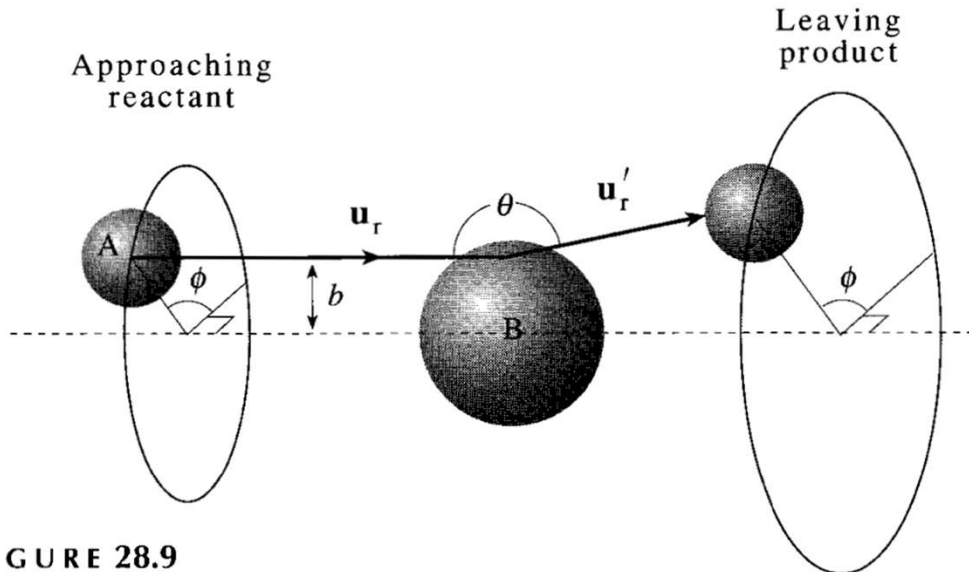


FIGURE 28.9

The angular distribution resulting from the bimolecular collision between molecules A and B as seen from the B molecule before and after the collision. For a fixed value of b , the impact parameter, the reactants and products take on all possible angles ϕ with equal probability, thereby forming a cone around the relative velocity vector \mathbf{u}_r . The angle θ , however, depends on the dynamics of the reaction and must be determined experimentally.

Figure 28.5 shows a series of snapshots of a bimolecular collision as viewed along the motion of the center of mass. Figure 28.5 implies that the center-of-mass motion is constant during the entire collision. The relative velocity, on the other hand, changes during the collision. The colliding molecules move in the plane defined by 1234, which itself is moving at the velocity of the center of mass.

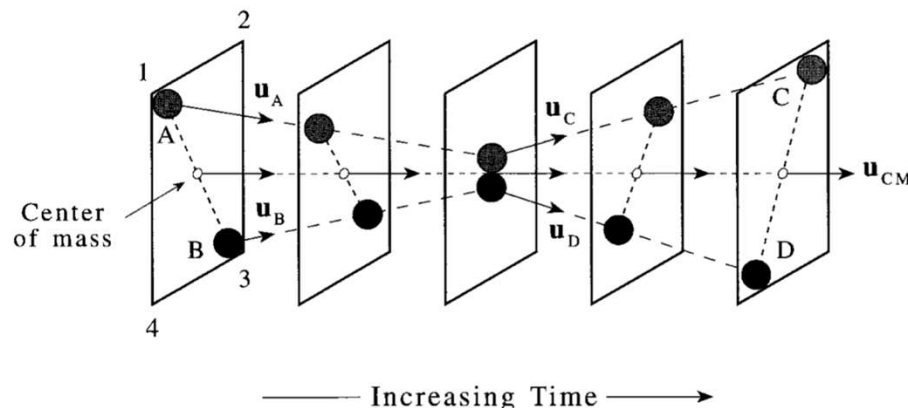


FIGURE 28.5

The details of a bimolecular collision viewed at various times along the center-of-mass motion. The velocities of the reactants A and B and products C and D can be divided into a component that lies along the center of mass and a relative velocity component that lies in the plane defined by 1234. The center-of-mass velocity remains constant before, during, and after the collision, and therefore the molecules remain in a plane that travels at the speed of the center of mass. Only the relative component of the velocity is important in determining the energy available for the reaction. In the left two snapshots, molecules A and B are approaching one another in the 1234 plane. The collision occurs in the middle snapshot. The right two snapshots show the products moving apart in the 1234 plane. The direction of the relative velocity of the reactants and products can be different.

The maximum or terminal velocity of molecules in a supersonic beam can be determined by assuming that all of the internal energy of the molecules inside the source is converted into kinetic energy directed along the beam axis, in an *isenthalpic* expansion (i.e. $\Delta H = 0$ during the expansion). Assuming ideal gas behaviour, we have

$$\frac{1}{2} mu^2 = - \int_{T_s}^{T_f} C_p dT \quad (1)$$

where $\frac{1}{2} mu^2$ is the kinetic energy of the beam molecules and $C_p dT = dH$ is the change in enthalpy of the molecules within the source as they undergo supersonic expansion. T_s and T_f are the temperatures of the source and molecular beam, respectively. Since T_f is small relative to T_s , we have $T_s - T_f \approx T_s$. Also, assuming C_p is not temperature dependent, we can set $C_p = \gamma R / (\gamma - 1)$, where $\gamma = C_p / C_v$. Evaluating (1) then gives

$$\frac{1}{2} mu^2 = \left(\frac{\gamma R}{\gamma - 1} \right) T_s \quad (2)$$

Rearranging yields the beam terminal velocity.

$$u = \left(\frac{2RT_s}{m(\gamma-1)} \right)^{1/2} \quad (3)$$

We see from Equation (3) that the terminal velocity of a supersonic molecular beam depends on the mass of the beam gas, with light gases achieving higher speeds than heavier gases. A beam of He has a terminal velocity of around 2400 ms^{-1} , while for HCl it is much lower, at around 500 ms^{-1} . Higher beam velocities for heavier molecules may be achieved by ‘seeding’ the heavier molecule in a light carrier gas so as to achieve a lighter ‘average mass’ for the beam molecules; a beam of 1% HCl in He, for example, has a terminal velocity of around 2100 ms^{-1} .

The velocity of the DF(g) molecule depends on the vibrational state of the product. This means that in a crossed molecular beam apparatus, the time required for the DF(g) molecule to travel from the collision region to the mass spectrometer will depend on its vibrational state. Figure 28.10 illustrates the type of data observed if the mass spectrometer signal is plotted as a function of time. The graph reveals four distinguishable peaks. These four peaks correspond to product molecules that traveled away from the reaction site in the same direction but with different speeds, and therefore arrived at the mass spectrometer at different times. The first peak corresponds to those molecules that left the reaction site with the highest speed. These molecules have the largest translational energy and therefore the least amount of internal vibrational energy. Subsequent peaks correspond to molecules with a smaller translational energy and greater internal vibrational energy. The area under a peak is proportional to the total number of product molecules in that vibrational state. If we compare the areas of the different peaks, the relative populations of the different vibrational states can be determined.

The dependence of reaction product formation on the angle θ (shown in Figure 28.9) can be determined by moving the detector in the plane defined by the two molecular beams (see Figure 28.6a). Thus, we can determine the relative populations of each vibrational state for all possible scattering angles.

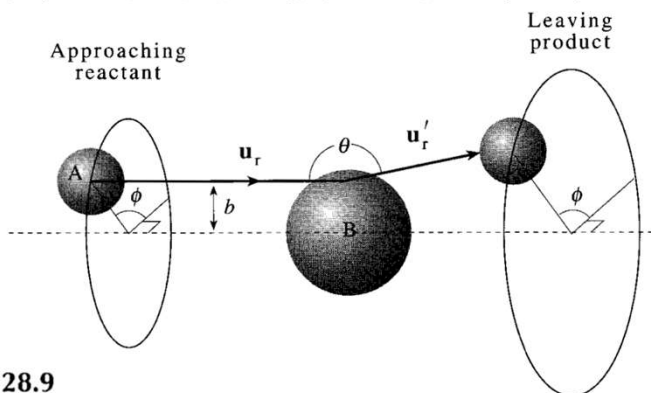


FIGURE 28.9
The angular distribution resulting from the bimolecular collision between molecules A and B

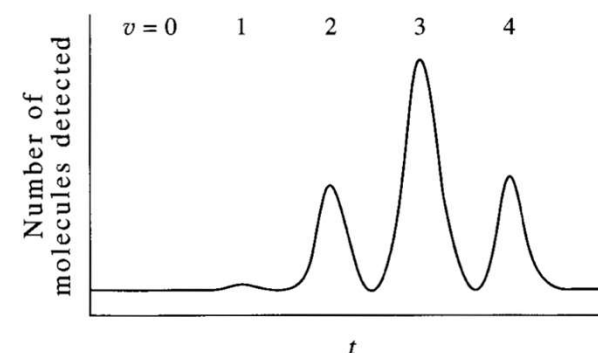


FIGURE 28.10

The number of DF(g) molecules detected by a mass spectrometer is plotted as a function of time after the reaction between F(g) and D₂(g) in a crossed molecular beam study. The initial relative kinetic energy of the reactants is 7.62 kJ·mol⁻¹. The DF(g) molecules with the highest translational energy, and therefore the least amount of vibrational energy, arrive at the detector first. Because the total energy is constant, DF(g) molecules produced in an excited vibrational state must have a lower translational energy. Therefore, the different peaks observed in the plot correspond to DF(g) molecules in different vibrational states. There is no peak at $v = 0$ because no DF(g) molecules are produced in the $v = 0$ vibrational state under these conditions.

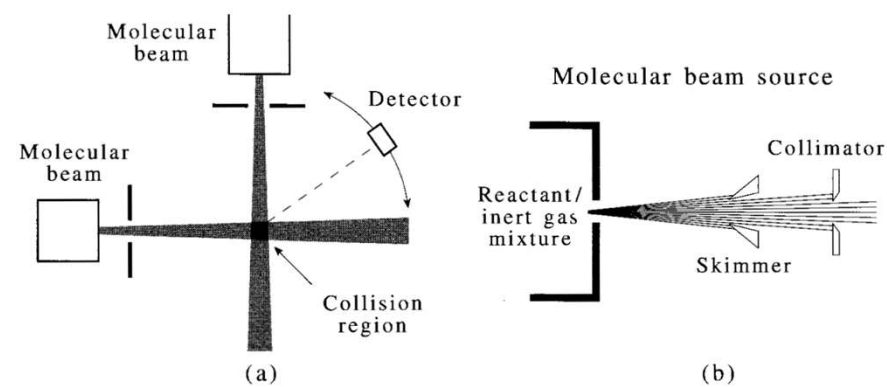
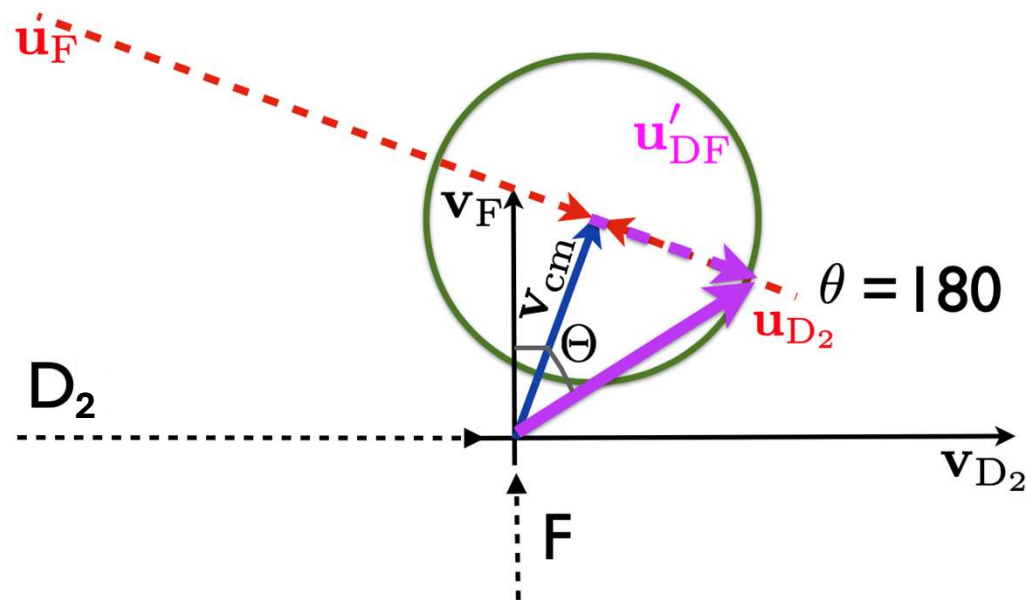
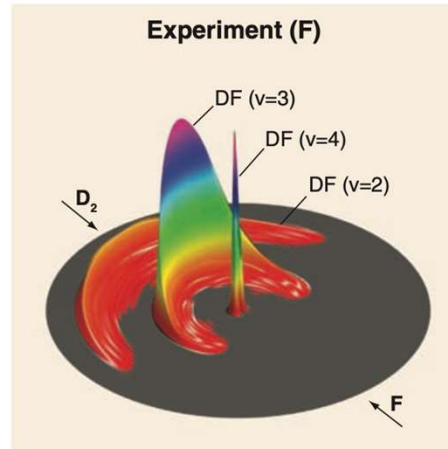
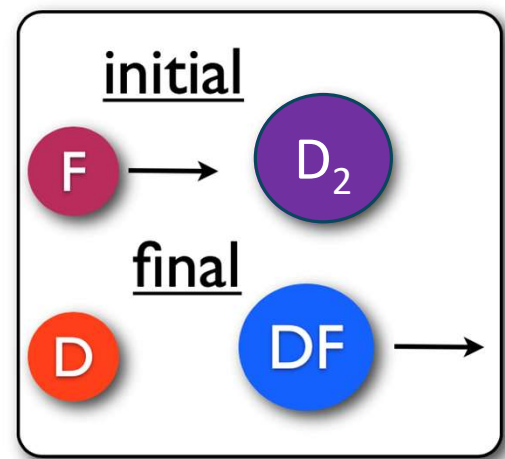


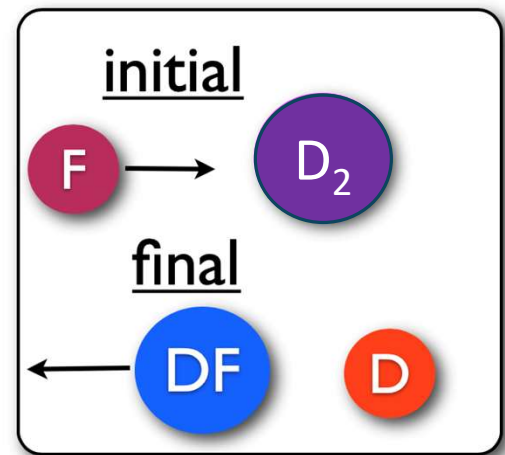
FIGURE 28.6
(a) A schematic diagram of a crossed molecular beam machine. Each reactant is introduced

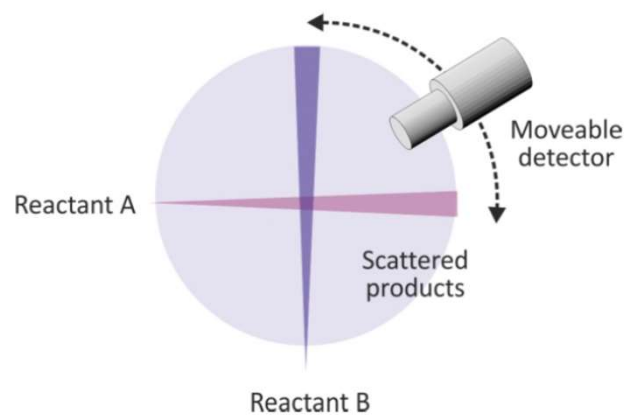


$$\theta = 0^\circ$$



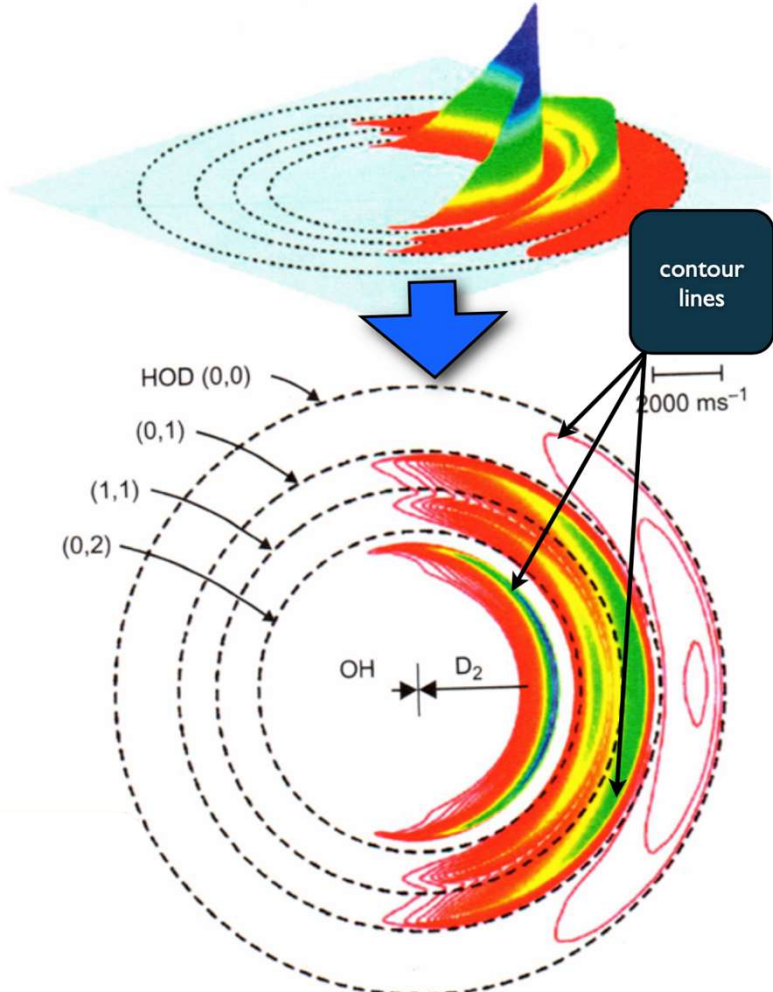
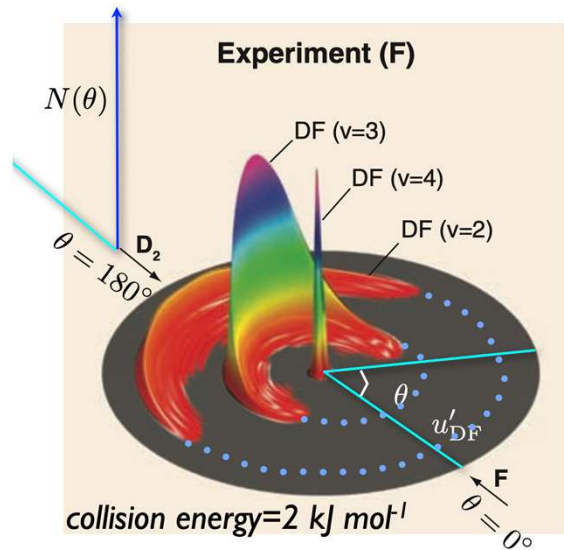
$$\theta = 180^\circ$$

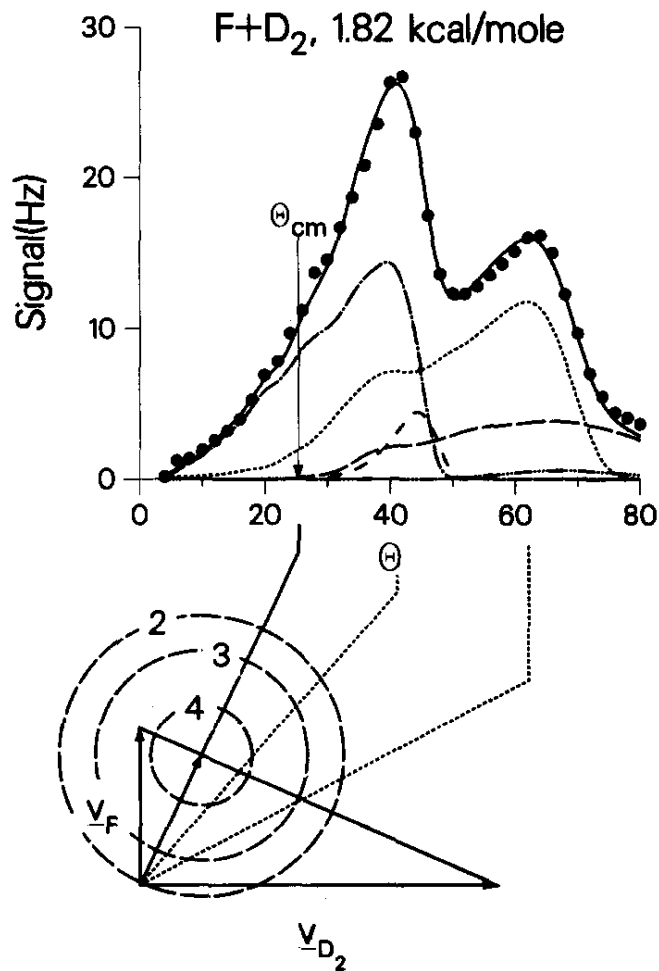
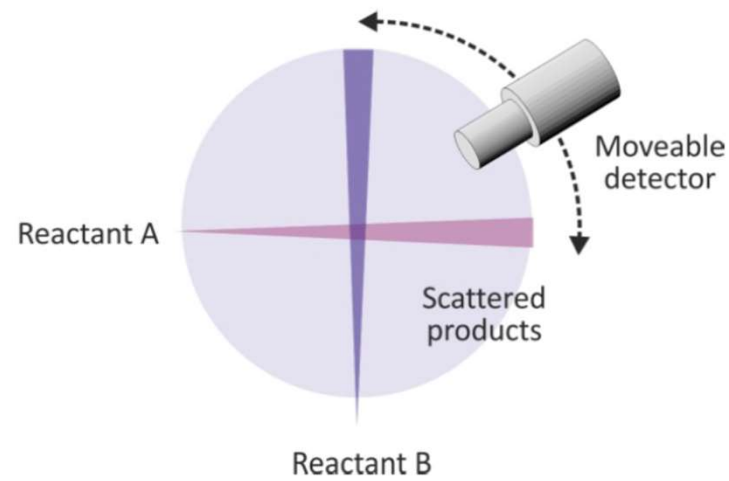




Rather than in a three-

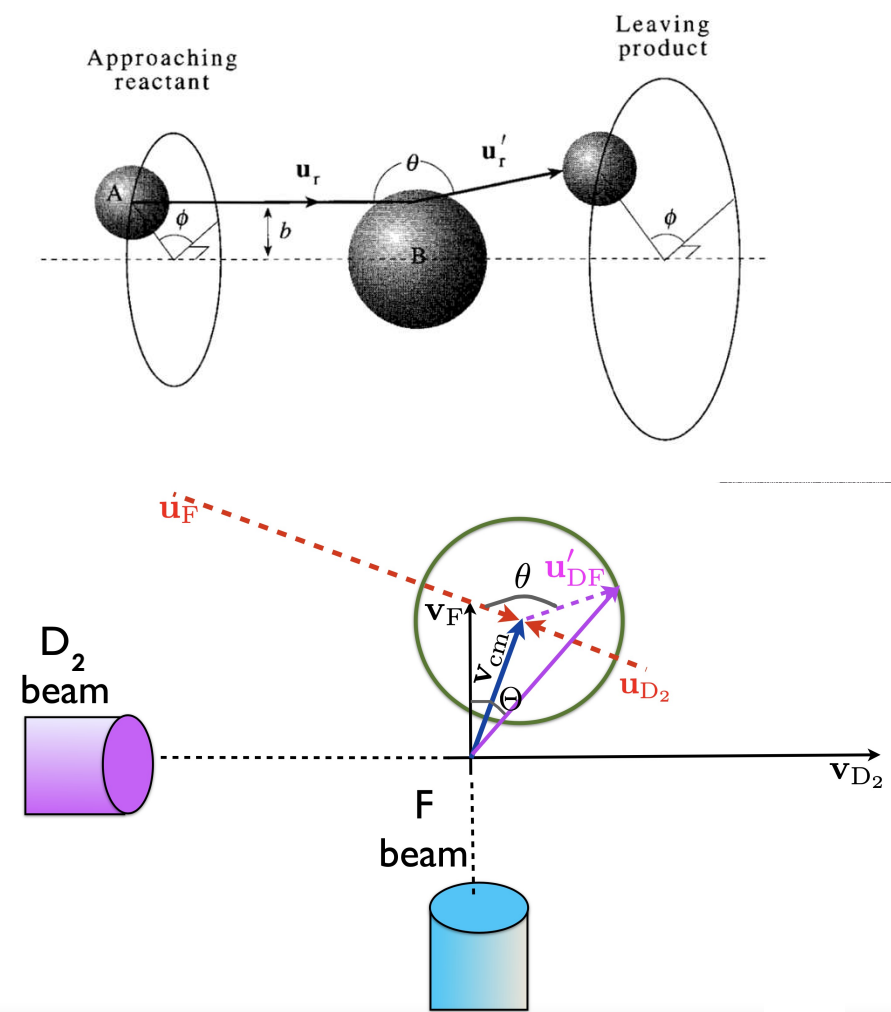
dimensional picture that depicts all the reaction trajectories, the data are commonly represented in a two-dimensional polar contour plot.



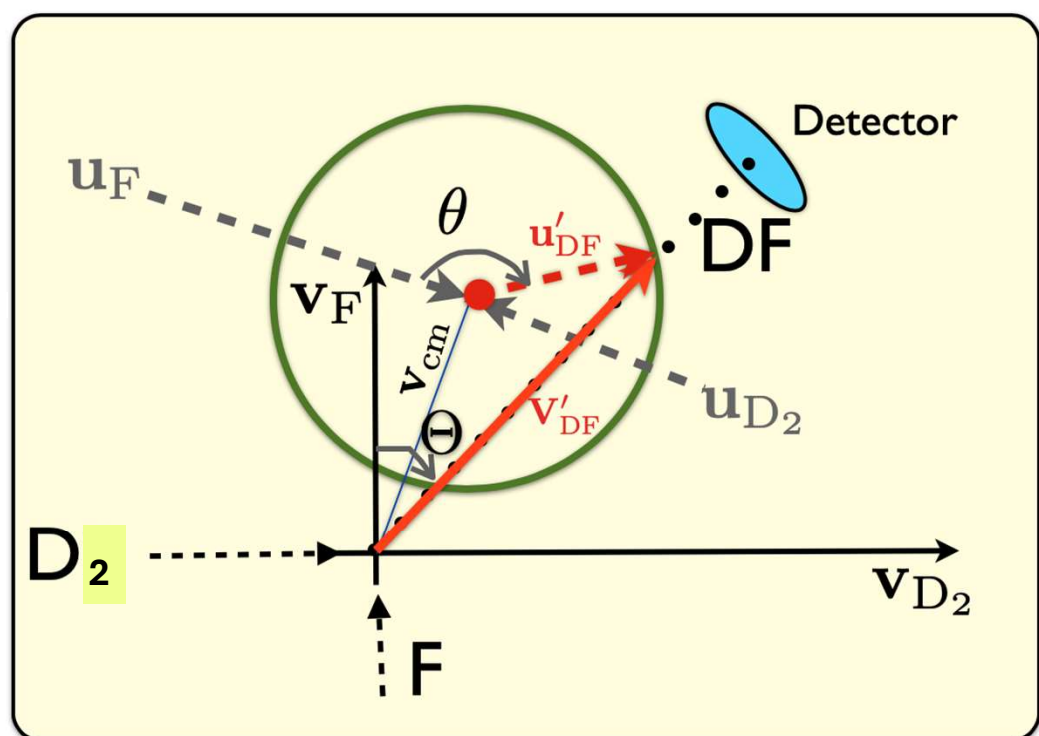


Neumark et al *J. Chem. Phys.* **1985**, *82*, 3067

Scattering Angle of Products

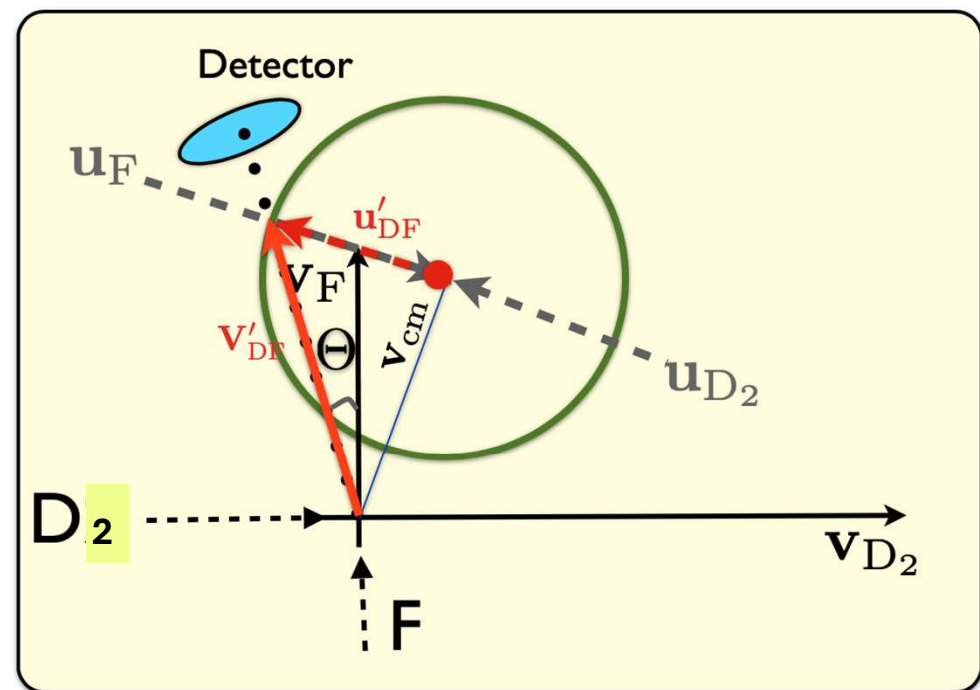
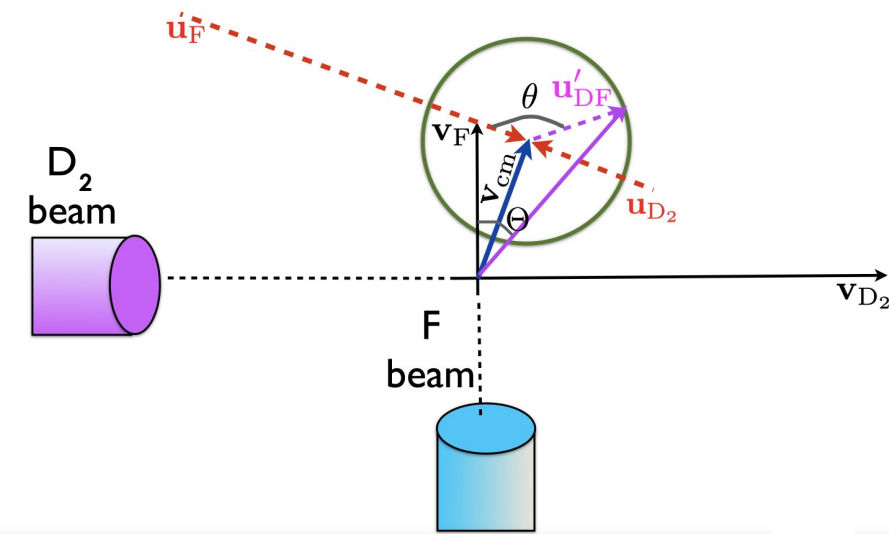


A general case for which $\theta < 180^\circ$



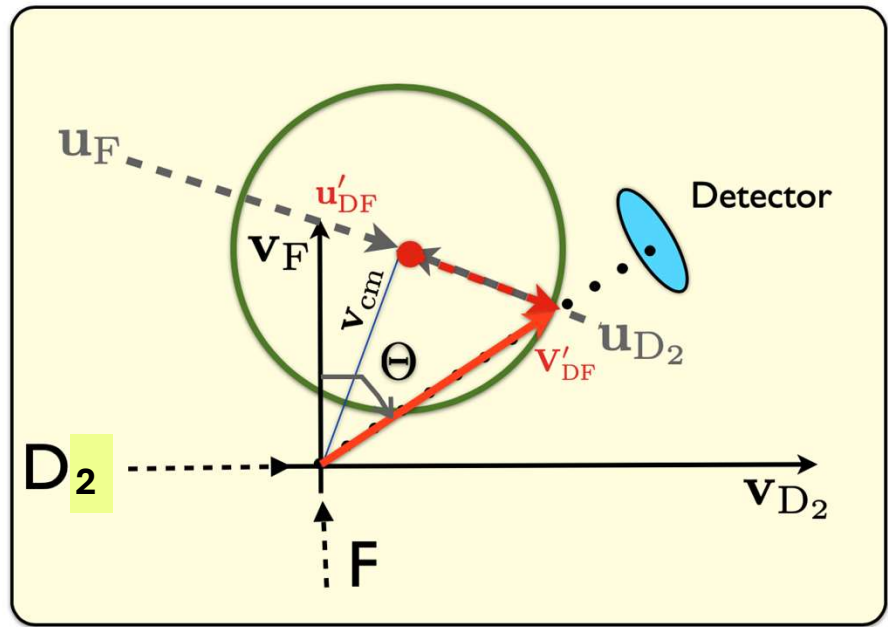
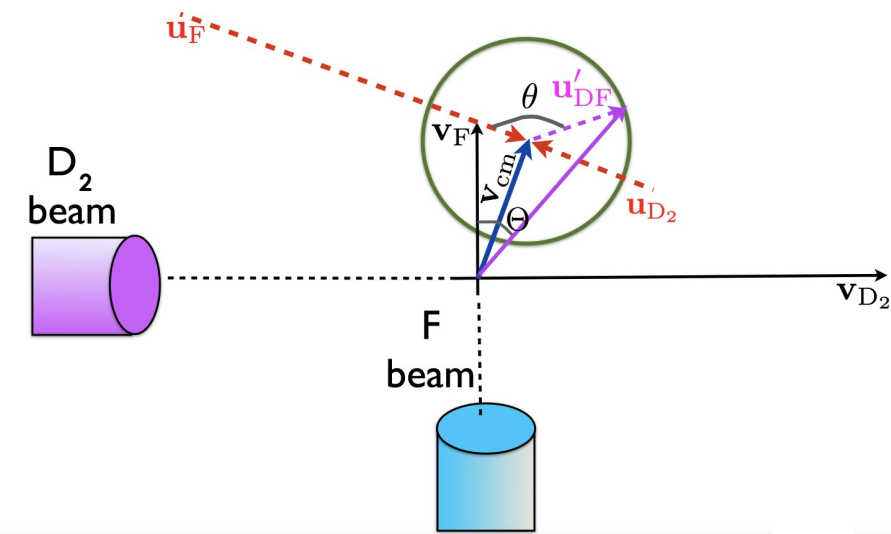
Scattering Angle of Products

A general case for which $\theta=0$



Scattering Angle of Products

A general case for which $\theta=180$



In the case of F+D₂ (Lee's expt), most of the DF products are with theta=180;
i.e. the above case.

Figure 28.11 shows the contour plot for the reaction between F(g) and D₂(v = 0), for which the relative translational energy of the reactants is 7.62 kJ·mol⁻¹. The center of mass sits at the center of the contour plot. The distance from the origin to any point in the polar plot is the speed of the DF(g) molecule relative to the center of mass, | $\mathbf{u}_{\text{DF}} - \mathbf{u}_{\text{cm}}$ |. Below the plot, the arrows indicate the directions with which the reactants approach each other. The horizontal axis of the contour plot lies along the relative velocity vector of the reactants. The angles indicated in Figure 28.11 are the scattering angles θ . In an atom-molecule reaction, we take $\theta = 0^\circ$ to lie along the direction defined by the trajectory of the incident atom. An angle of $\theta = 0^\circ$ corresponds to a collision in which the F(g) atom collides with the D₂(g) molecule and the DF(g) product molecule travels in the same direction as the incident F(g) atom. An angle of $\theta = 180^\circ$ corresponds to a collision in which the F(g) atom collides with the D₂(g) molecule, reacts, and then the DF(g) molecule bounces back opposite to the incident direction of the F(g) atom (Figure 28.12).

The contours in Figure 28.11 represent a constant number of DF(g) product molecules. The dashed circles in Figure 28.11 correspond to the maximum relative speed allowed for a product molecule in a given vibrational state. An increase in the diameter of this circle corresponds to an increase in the relative speed of the product molecule. Recall that the total energy is fixed, so the speed of the DF(g) molecule decreases with increasing vibrational quantum number. Thus, the diameters of the circles decrease with increasing vibrational quantum number. Notice that the data show that a large number of product molecules have speeds between the dashed circles. The dashed circles shown in Figure 28.11 correspond to the case where there is internal energy only in the vibrational states of the molecule, in which case the rotational energy corresponding to these circles is $E_{\text{rot}} = 0$, with $J = 0$. If DF(g) is produced in an excited rotational state, we would expect to observe a speed that has an value intermediate between two of the dashed circles. For example, the region between the dashed circles labeled $v = 3$ and $v = 4$ in Figure 28.11 (see point A in the figure) corresponds to a DF(g) molecule that has a vibrational quantum number $v = 3$ but is also rotationally excited. If we know the energy spacing of the rotational states, the rotational energy distribution can also be determined from the contour map.

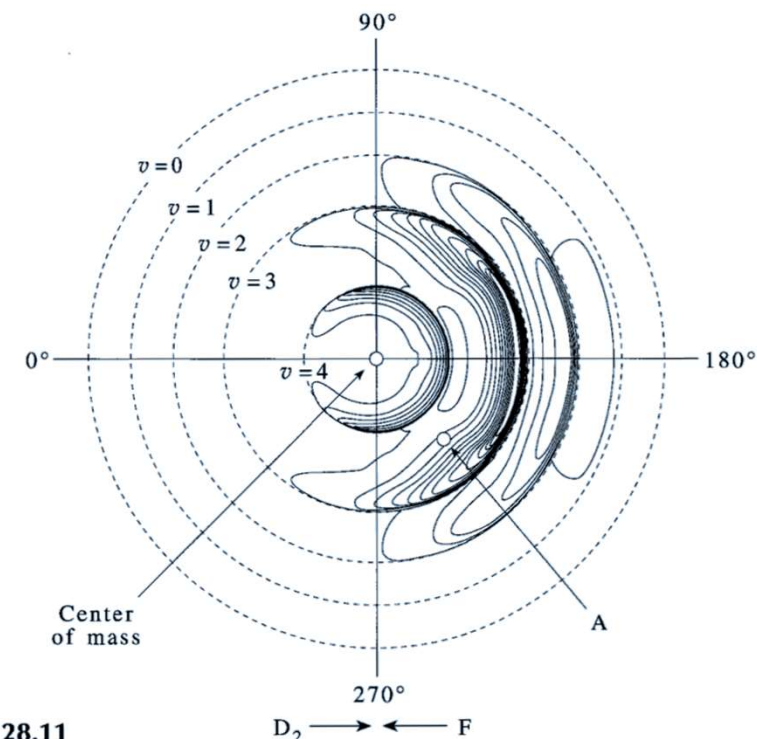


FIGURE 28.11

A contour map of the angular and speed distributions for the product molecule DF for the reaction F(g) + D₂(v = 0), for which the relative translational energy of the reactants is 7.62 kJ·mol⁻¹. The center of mass is fixed at the origin. The dashed circles correspond to the maximum relative speeds a DF(g) molecule can have for the indicated vibrational state. The data reveal that the product molecules preferentially scatter back in the direction of the incident fluorine atom, a scattering angle of $\theta = 180^\circ$. The arrows at the bottom of the figure show the direction with which each reactant molecule approaches each other.

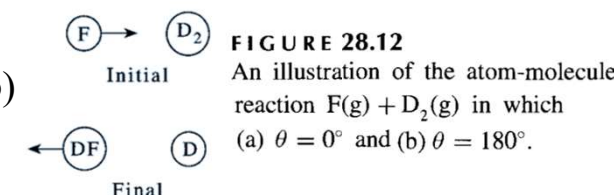
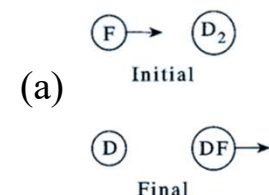
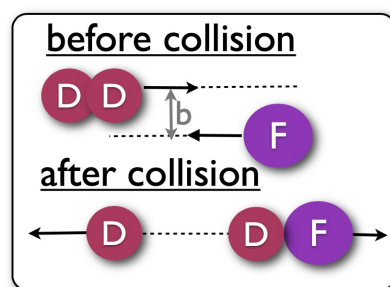


FIGURE 28.12

An illustration of the atom-molecule reaction F(g) + D₂(g) in which (a) $\theta = 0^\circ$ and (b) $\theta = 180^\circ$.

The experimental data in Figure 28.11 reveal three important features of the reaction. First, we see that the product preferentially scatters backward, toward the direction of the incident fluorine atom, a scattering angle of $\theta = 180^\circ$. These data suggest that the fluorine atom undergoes a nearly head-on collision with the $D_2(g)$ molecule and then bounces backward after abstracting one of the deuterium atoms. This type of reaction is called a *rebound reaction*. Second, an analysis of this contour map reveals that the most probable product of the reaction is $DF(v = 3)$. Third, there is considerable population between the dashed circles, indicating that a variety of rotational levels of the $DF(g)$ molecule are populated by the reaction.

The relative populations of the first five vibrational states deserve a bit more attention. Note the lack of contour lines between the dashed circles for $v = 0$ and $v = 1$. This result means that no product molecules are formed in the ground vibrational state. This product distribution cannot be described by a Boltzmann distribution and we say that the reaction generates a nonequilibrium product distribution.



$D_2 + F$ is a backward scattering/rebound reaction. Thus this reaction should occur with **small values of b**

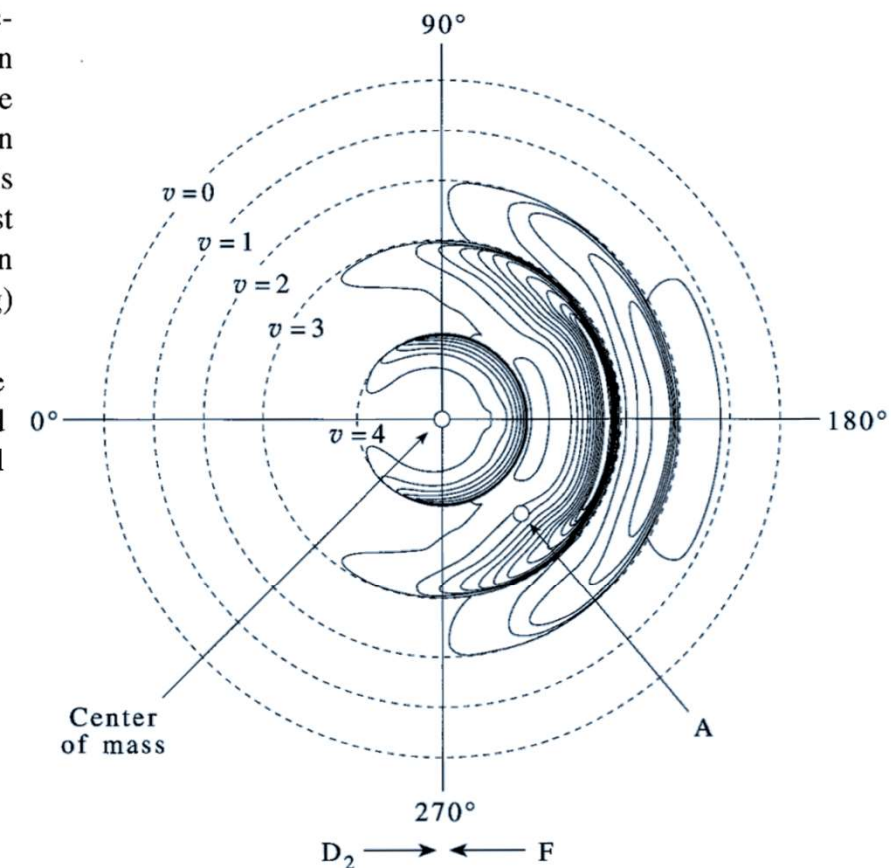
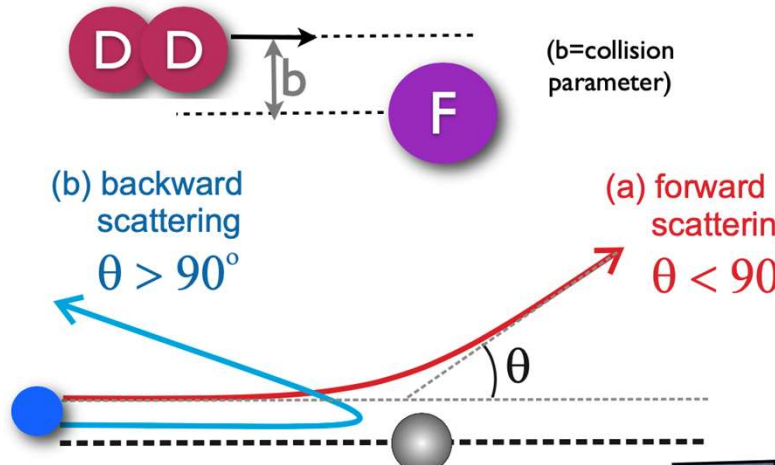


FIGURE 28.11

A contour map of the angular and speed distributions for the product molecule DF for the reaction $F(g) + D_2(v = 0)$, for which the relative translational energy of the reactants is $7.62 \text{ kJ} \cdot \text{mol}^{-1}$. The center of mass is fixed at the origin. The dashed circles correspond to the maximum relative speeds a $DF(g)$ molecule can have for the indicated vibrational state. The data reveal that the product molecules preferentially scatter back in the direction of the incident fluorine atom, a scattering angle of $\theta = 180^\circ$. The arrows at the bottom of the figure show the direction with which each reactant molecule approaches each other.

Classical Scattering Theory: Forward vs backward scattering



The following figure explains the classical scattering. If the collision is nearly head-on, i.e. for smaller values of b [blue line], classical scattering says that the collision should result in backward scattering. On the other hand, if the collision is for higher values of b [red curve], the scattering should be forward scattering.

backward scattering/
rebound reaction is caused
by collisions having
small values of b

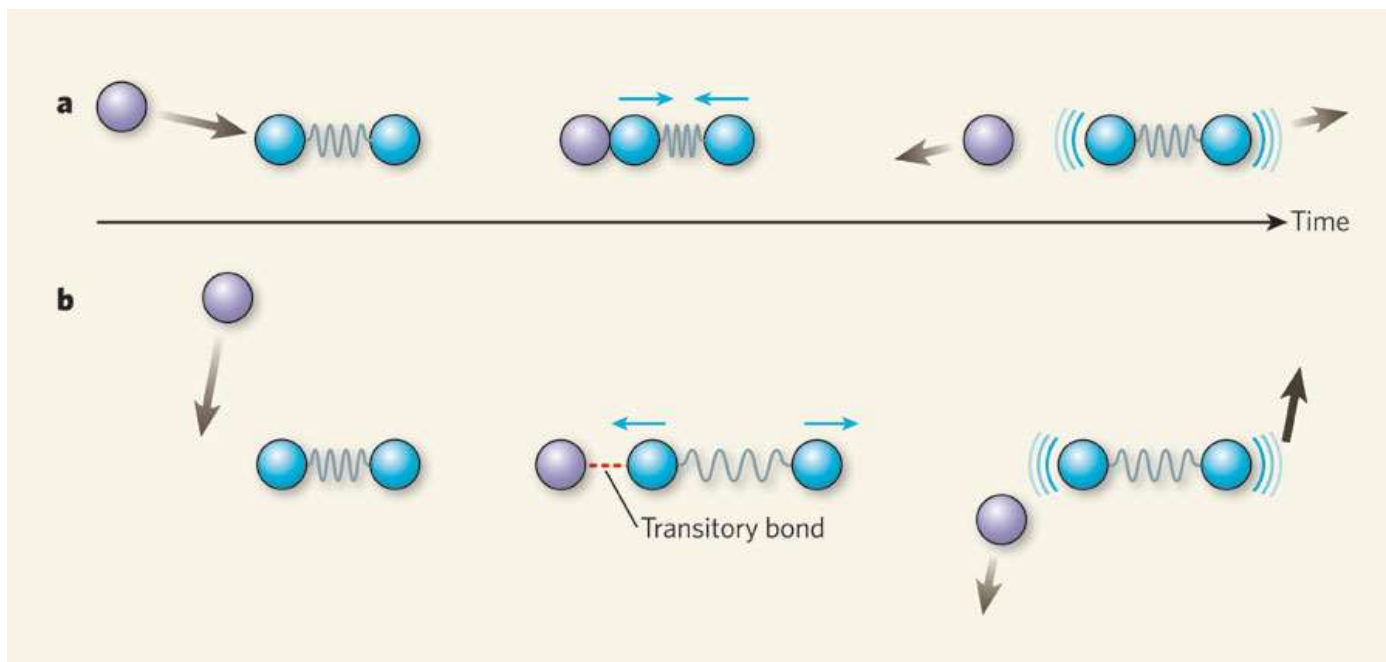
forward scattering/
stripping reaction is
caused by collisions having
large values of b

PHYSICAL CHEMISTRY

When molecules don't rebound

Mark Brouard

Picture a simple molecule as two balls attached together by a compressible spring. If an incoming atom strikes one end of the molecule, the spring compresses and the vibrating molecule jumps backwards. Or does it?



28–9. Not All Gas-Phase Chemical Reactions Are Rebound Reactions

Figure 28.13 shows the velocity contour map for the reaction



in which the initial relative translational energy between the reactants is $15.13 \text{ kJ} \cdot \text{mol}^{-1}$. Unlike in the $\text{F(g)} + \text{D}_2\text{(g)}$ reaction, we can see that the product diatomic molecule in this case, KI(g) , is preferentially scattered in the forward direction, along the direction of the incident K(g) atom. This type of reaction, in which the incident atom abstracts part of a molecule and keeps going in the forward direction, is called a *stripping reaction*.

The mechanism of stripping reactions is interesting. The reaction cross section for the $\text{K(g)} + \text{I}_2\text{(g)}$ reaction is $1.25 \times 10^6 \text{ pm}^2$. Assuming the radius of K(g) and $\text{I}_2\text{(g)}$ are 205 pm and 250 pm, respectively, the hard-sphere collision cross section is $\pi d_{AB}^2 = 6.5 \times 10^5 \text{ pm}^2$. The measured reaction cross section is twice as large as the hard-sphere estimate. If the approaching potassium atom and iodine molecule were to travel in straight lines at the maximum impact parameter corresponding to this experimentally determined reaction cross-section, these reactants would miss one another. The fact that a reaction occurs indicates that the trajectories of the reacting molecules are affected by a long-range potential that draws them together. We would not expect the van der Waals interactions between the potassium atom and the iodine molecule to be strong enough to cause such a large effect. Research shows that this reaction involves the transfer of an electron between the two reactants, which takes place before the reactants collide. Thus, the first step of the reaction occurs when the reactants are still separated and produces a pair of ions,



The ions are then attracted to one another through a Coulomb potential. The more energetically stable products $\text{KI(g)} + \text{I(g)}$ are formed when the two ions collide. The KI(g) moves off in the same direction as the incident potassium ion. This mechanism has been coined the *harpoon mechanism* because the potassium atom uses its electron like a harpoon to draw in the $\text{I}_2\text{(g)}$ molecule.

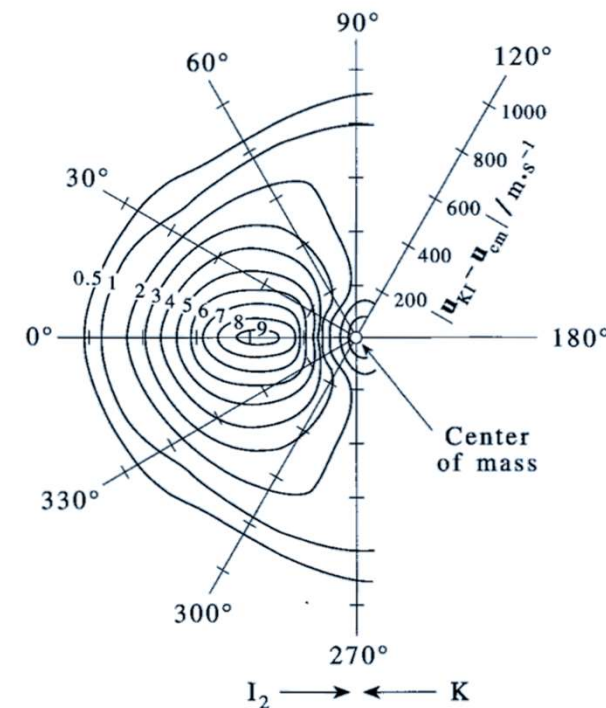
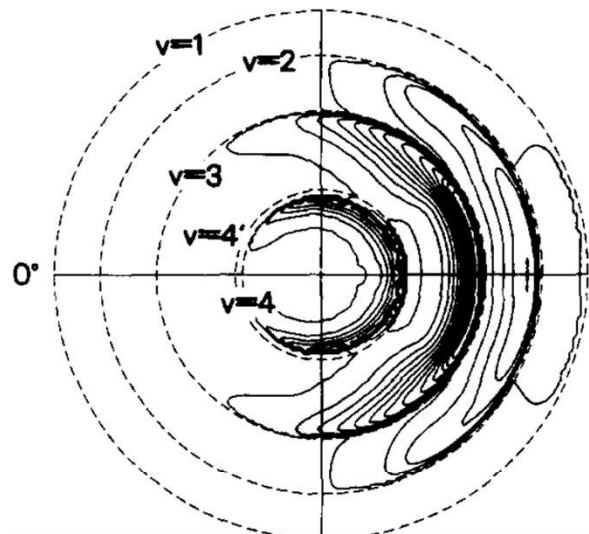
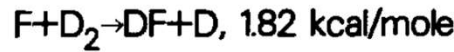


FIGURE 28.13

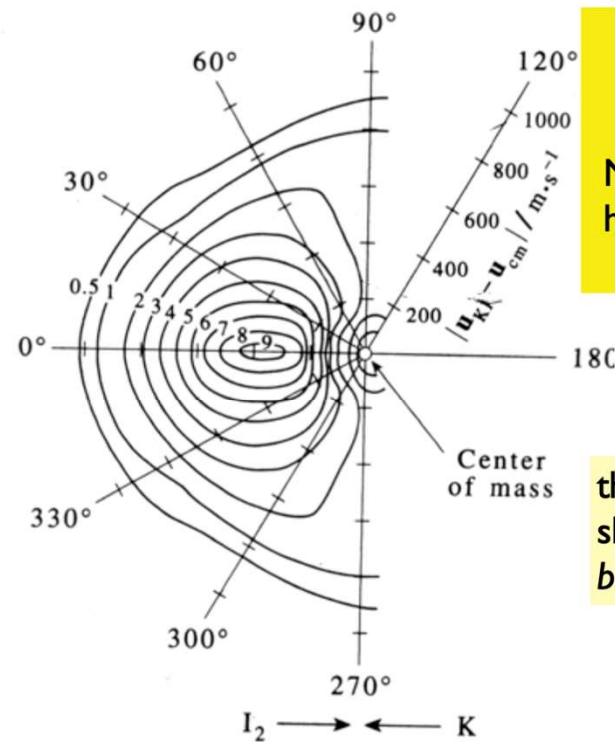
A contour map of the angular and velocity distributions for the product molecule KI(g) for the reaction $\text{K(g)} + \text{I}_2\text{(g)} \rightarrow \text{KI(g)} + \text{I(g)}$, in which the relative translational energy of the reactants is $15.13 \text{ kJ} \cdot \text{mol}^{-1}$. In this stripping reaction, the product molecules continue going in the direction of the incident potassium atom, a scattering angle near $\theta = 0^\circ$. The numbers that label the contours are a measure of the relative number of KI(g) molecules.

Rebound & Stripping Mechanisms



This is an example of **rebound reactions**:
Newton's diagram has theta=180 highly populated

this reaction should have small b



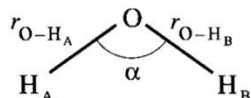
This is an eg. of **stripping reaction**.
Newton's diagram has theta=0 highly populated

this reaction should have high b

28–10. The Potential-Energy Surface for the Reaction $F(g) + D_2(g) \Rightarrow DF(g) + D(g)$ Can Be Calculated Using Quantum Mechanics

In Chapter 9, we learned that the potential energy of a diatomic molecule depends on only the distance between the two bonded atoms. Thus, the potential-energy surface for a diatomic molecule such as $D_2(g)$ or $DF(g)$ can be plotted in two dimensions by plotting the potential energy as a function of the bond length. The word “surface” is a misnomer in this case. A diatomic molecule has only one geometric parameter, the bond length. Using the term “potential-energy curve” when the potential energy depends on a single parameter and the word “surface” when the potential energy depends on more than one geometric parameter is more appropriate. Figure 28.15 shows the potential-energy curve for $D_2(g)$.

The potential energy of a polyatomic molecule depends on more than one variable because there is more than one bond length that can be varied. We will also need to specify the bond angle(s). For example, consider a water molecule. The geometry of a water molecule is completely specified by three geometric parameters, r_{O-H_A} , r_{O-H_B} , and the angle α between the two O–H bonds.



The potential energy of a water molecule is a function of these three parameters, or $V = V(r_{O-H_A}, r_{O-H_B}, \alpha)$. A plot of the complete potential-energy surface of a water molecule therefore requires four axes, one axis for the value of the potential energy and one axis for each of the three geometric parameters. The potential-energy surface is four-dimensional. Because we are limited to three dimensions for plotting functions, we cannot draw the entire potential-energy surface of a water molecule in a single plot.

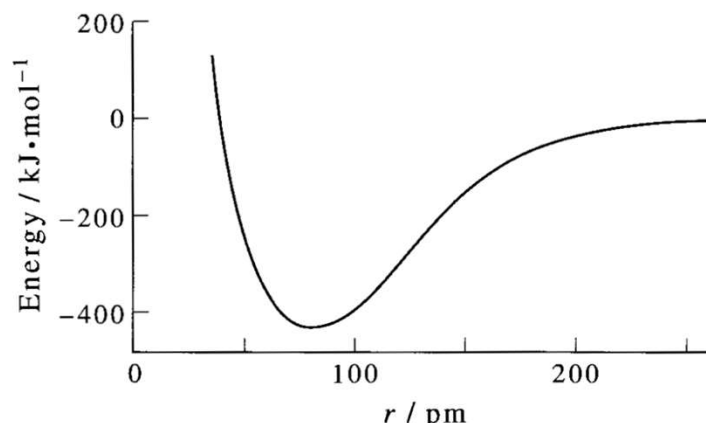


FIGURE 28.15

The potential-energy curve of $D_2(g)$. The zero of energy is defined to be that of the two separated atoms. The minimum of the potential-energy curve corresponds to the equilibrium bond length of the $D_2(g)$ molecule.

We can, however, draw parts of the potential-energy surface. We can fix one of the geometric parameters, for example, the angle α , and then draw a three-dimensional plot of $V(r_{O-H_A}, r_{O-H_B}, \alpha = \text{constant})$. Such a plot is a cross-sectional cut of the full potential-energy surface. A cross-sectional plot teaches us how the potential energy of the molecule changes when we vary some of the geometric variables while holding others constant. For example, a three-dimensional plot of $V(r_{O-H_A}, r_{O-H_B}, \alpha = \text{constant})$ as a function of r_{O-H_A} and r_{O-H_B} tells us how the potential energy of a water molecule changes when the bond lengths r_{O-H_A} and r_{O-H_B} are varied at a constant bond angle of α . If we made a series of cross-sectional plots for different values of α , we could see how the potential energy depends upon the bond angle.

Intricacies of Y.T. Lee's Experiments that we have pinpointed

1. Why is the $D_2 + F$ reaction rebound?
2. Why is there a forward flux seen when the collision energy is increased? Why is this forward flux only observed for $v=4$?
3. Why is the population of the DF products higher for $v=3$ (and $v=4$ for some collisional energy)?